Deep-learning-augmented Physics Models to Predict Nonlinear Dynamic Responses of Multi-degree-of-freedom Structures

Jaehwan Jeon
Graduate Student, Dept. of Civil and Environmental Engineering, Seoul National University, Seoul, South Korea

Junho Song
Professor, Dept. of Civil and Environmental Engineering, Seoul National University, Seoul, South Korea

ABSTRACT: Predicting a structure's dynamic response is essential in system identification, structural health monitoring, and structural reliability assessment. In recent years, many deep-learning-based methods have been developed to predict the dynamic responses of structures based on measurement data while guided by physics-based knowledge. However, such an approach has not yet been applied to predict the nonlinear dynamic responses of a large degree-of-freedom (DOF) structure. In this paper, the neural-network-augmented physics (NNAP) model is further developed to incorporate information on multi-degree-of-freedom structural systems by transforming the original DOF into a low-dimensional system using modal truncation. The prediction performance of the proposed method is verified through the numerical example of the Lysefjord bridge structure subjected to response-dependent wind loads. The proposed method is expected to promote further developments of physics-based deep learning approaches for complex structures with large DOFs.

1. INTRODUCTION

In system identification and structural health monitoring, engineers often aim to detect anomalies in the system by comparing the responses predicted based on a physics-based model and the actual responses measured from the structure. Therefore, an accurate model for predicting the dynamic response is crucial for successful outcomes. From the structural reliability perspective, epistemic uncertainties in a physics-based model and its parameters may lead to a significant risk of making improper engineering decisions.

Encouraged by the fast development of deep learning and a large amount of data, researchers have tried to incorporate physics-based knowledge into deep learning models trained by data. Such physics-based deep learning methods have been getting attention since they can help the model avoid overfitting by incorporating the physics information of the structures during the training and the predicting scheme. For example, Zhang et al. (2020) predicted the dynamic response of structures subject to earthquake ground motions using the physics-guided convolutional neural network in which physical constraints are imposed through the physics-guided loss function. Eshkevari et al. (2021) designed a neural network architecture similar to the time-integration scheme of the equation of motion.

Another approach in physics-based deep learning is the hybrid modeling of existing physics models and neural networks. These hybrid models have been widely applied in civil and mechanical engineering fields. For example, Kim et al. (2012) constructed a hybrid model for the bolted flange-plate connection. Punjani and Abbeel (2015) described a helicopter dynamics system by modeling the unknown linear and angular acceleration by the quadratic lag model and a neural network and combining it with the known dynamics of gravity and the kinematics of rotation.

However, these physics-based deep learning models have not yet been applied to predict the responses of a large degree-of-freedom (DOF) structure. This is challenging because many physics-based deep learning models softly impose the physical constraints by a single loss function, which may not ensure the prediction accuracy over many DOFs all at once.

This study aims to develop a deep-learning-augmented physics-based model to predict the nonlinear dynamic responses of multi-degree-of-freedom (MDOF) structures. The method is mainly based on the hybrid modeling of a physics-based model and a neural network. Specifically, the neural-network-augmented physics (NNAP) model (De Groote et al. 2022) is further developed by transforming the model into one with reduced coordinates. The effect of the modal truncation introduced during the transformation on the performance of the proposed method is investigated by its application to a bridge structure subject to nonlinear response-dependent wind-induced input forces.

2. STRUCTURAL SYSTEMS SUBJECT TO RESPONSE-DEPENDENT FORCES

2.1. Equation of motion

Consider an N DOF nonlinear structural system subject to response-dependent dynamic forces. The equation of motion for the structural system can be described as

$$\mathbf{M}\ddot{\boldsymbol{x}} + \mathbf{F}_{\mathbf{I}}(\boldsymbol{x}, \dot{\boldsymbol{x}}) = \mathbf{F}(\boldsymbol{x}, \dot{\boldsymbol{x}}, \boldsymbol{p}) \quad (1)$$

where $\boldsymbol{x}$, $\dot{\boldsymbol{x}}$, and $\ddot{\boldsymbol{x}}$ respectively denote the displacement, velocity, and acceleration of the structure, $\mathbf{M}$ denotes the mass matrix, $\mathbf{F}_{\mathbf{I}}$ denotes the internal force vector, $\mathbf{F}$ is the dynamic external force vector, and $\boldsymbol{p}$ is the vector process describing the source excitation of the dynamic external force. For example, if an earthquake ground acceleration $\ddot{x}_g$ is applied as an external force, then $\boldsymbol{p} = p = \ddot{x}_g$ and $\mathbf{F}(\boldsymbol{x}, \dot{\boldsymbol{x}}, \boldsymbol{p}) = -\boldsymbol{M}\boldsymbol{\upsilon}\boldsymbol{p}$ where $\boldsymbol{\upsilon}$ denotes the influence vector which converts the planar ground motion to the effective ground motion. In Eq. (1), the displacement and velocity of the structure are taken as inputs of the external force vector $\mathbf{F}$ to show the response-dependence of the loads. For example, the wind load in the along-wind direction for a one-dimensional 1DOF structure can be expressed as $\mathbf{F}(\boldsymbol{x}, \dot{\boldsymbol{x}}, \boldsymbol{p}) = F(x, \dot{x}, p) = 1/2\, \rho C_D A_D (u - \dot{x})^2$ where p represents the along-wind velocity u, ρ denotes the air density, and C_D and A_D each denotes the drag coefficient and the effective surface area subject to the wind force.

In general, dynamical systems can be represented by a state-space formulation, which is generally given as

$$\dot{\mathbf{X}} = \mathbf{f}(\mathbf{X}, \boldsymbol{p}) \quad (2)$$

where $\mathbf{X}$ and $\dot{\mathbf{X}}$ denote the state vector and its time derivative, respectively. Defining the state vector as $\mathbf{X} = [\boldsymbol{x}^{\mathrm{T}}\ \dot{\boldsymbol{x}}^{\mathrm{T}}]^{\mathrm{T}}$, the state-space form of Eq. (1) is derived as

$$\dot{\mathbf{X}} = \begin{bmatrix} \dot{\boldsymbol{x}} \\ \mathbf{M}^{-1}\big(\mathbf{F}(\boldsymbol{x}, \dot{\boldsymbol{x}}, \boldsymbol{p}) - \mathbf{F}_{\mathbf{I}}(\boldsymbol{x}, \dot{\boldsymbol{x}})\big) \end{bmatrix} \quad (3)$$

Formulating the equation of motion of the structure in a state-space format, as in Eq. (3), facilitates the application of NNAP models, as explained in Section 3.

2.2. Reduced order models by modal truncation

For an MDOF linear structural system, a reduced-order model can be constructed by modal truncation. The procedure starts by conducting the eigenvalue analysis

$$\det(\mathbf{M} - \lambda\mathbf{K}) = 0 \quad (4)$$

where $\mathbf{K}$ is the stiffness matrix of the linear system. Solving Eq. (4) for λ gives eigenvalues $\lambda_1, \lambda_2, \dots, \lambda_N$ and the corresponding eigenmodes $\boldsymbol{\phi}_1, \boldsymbol{\phi}_2, \dots, \boldsymbol{\phi}_N$. In the reduced-order model, the response $\boldsymbol{x}$ is assumed as a linear combination of N_r $(< N)$ mode shapes and the corresponding mode responses:

$$\boldsymbol{x} = \sum_{i=1}^{N_r} \boldsymbol{\phi}_i q_i = \mathbf{\Phi}_{\mathbf{r}}\boldsymbol{q} \quad (5)$$

where $\mathbf{\Phi}_{\mathbf{r}} = [\boldsymbol{\phi}_1\ \boldsymbol{\phi}_2 \dots \boldsymbol{\phi}_{N_r}]$, and $\boldsymbol{q}$ is the mode response vector constructed as $[q_1 \quad q_2 \quad \dots q_{N_r}]^{\mathrm{T}}$. The reduced order model by modal truncation can be expressed as

$$\mathbf{\Phi}_\mathrm{r}^\mathrm{T}\mathbf{M}\mathbf{\Phi}_\mathrm{r}\ddot{\boldsymbol{q}} + \mathbf{\Phi}_\mathrm{r}^\mathrm{T}\mathbf{K}\mathbf{\Phi}_\mathrm{r}\boldsymbol{q} = \mathbf{\Phi}_\mathrm{r}^\mathrm{T}\mathbf{F} \quad (6)$$

As for nonlinear structural systems, Slaats et al. (1995) proposed three mode types for reduced-order models. For example, among the three mode types, the tangent modes can be computed by linearizing the dynamical systems at the initial state:

$$\mathbf{K} = \left.\frac{\partial \mathbf{F}_\mathrm{I}}{\partial x}\right|_{x=x(0)} \quad (7)$$

Substituting Eq. (7) into Eq. (4) gives the set of linearized eigenmodes, which can be used to reduce the order of the system.

3. NEURAL-NETWORK-AUGMENTED PHYSICS (NNAP) MODEL

Consider a dynamical system that is described in the state-space format as in Eq. (3). If Eq. (3) is modeled only by the physics model $\boldsymbol{\mathcal{P}}$, the system can be expressed as

$$\dot{\mathbf{X}} = \boldsymbol{\mathcal{P}}(\mathbf{X}, \boldsymbol{p}) \quad (8)$$

However, if the system has unknown dynamics that the physics-based model cannot describe effectively, Eq. (8) may not identify model parameters or provide accurate predictions. In such cases, the hybrid model approach aims to complement the errors of the known dynamics model $\boldsymbol{\mathcal{P}}$ by adding the unknown physics model $\boldsymbol{\mathcal{U}}$ as follows:

$$\dot{\mathbf{X}} = \boldsymbol{\mathcal{P}}(\mathbf{X}, \boldsymbol{p}_1) + \boldsymbol{\mathcal{U}}(\mathbf{X}, \boldsymbol{p}_2) \quad (9)$$

where $\boldsymbol{p}_1 \cup \boldsymbol{p}_2 = \boldsymbol{p}$ and $\boldsymbol{\mathcal{U}}$ represents a data-driven model describing the unknown physics.

To describe a subset of Eq. (9) that the known physics model $\boldsymbol{\mathcal{P}}$ cannot describe, the outputs of a neural network $\boldsymbol{\eta}$ are augmented to the equations as

$$\dot{\mathbf{X}} = \boldsymbol{\mathcal{P}}(\mathbf{X}, \boldsymbol{p}_1) + \mathbf{R}\boldsymbol{\eta}(\mathbf{X}, \boldsymbol{p}_2; \boldsymbol{\theta}) \quad (10)$$

where $\mathbf{R}$ is a matrix consisting of 0's and 1's to specify the matches between the DOFs of the state-space form and the outputs of the network $\boldsymbol{\eta}$, and $\boldsymbol{\theta}$ is a set of the neural network parameters. Figure 1 illustrates the NNAP model in Eq. (10).

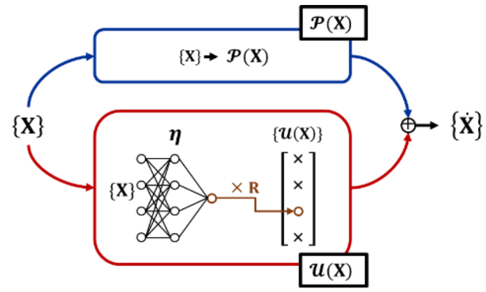

Figure 1: Illustration of NNAP model

In practice, only a subset of the state vector $\mathbf{X}$ is measurable or direct measurement is infeasible. In this study, assuming the measurement is a linear combination of the state vector, the vector $\mathbf{Y}$ with dimension $N_\mathrm{o}(< N)$ is introduced to denote the measured data, i.e.,

$$\mathbf{Y} = \mathbf{A}\mathbf{X} \quad (11)$$

If $\mathbf{Y}$ represents a set of direct measurements, $\mathbf{A}$ becomes a matrix consisting of 0's and 1's to indicate which response is measurable.

3.1. Procedures for prediction and training of NNAP model

A numerical time integration solver can solve the NNAP model described in Eq. (10) and Eq. (11). In other words, given the initial condition $\mathbf{X}_0$ of a structure, the response at the next time steps can be recurrently predicted from the previous time steps using a numerical solver such as Euler's method and the Runge-Kutta method.

Before predicting dynamic responses of a structure by the NNAP model, the neural network $\boldsymbol{\eta}$ in Eq. (10) needs to be properly trained. The backpropagation method can be applied to train the neural network $\boldsymbol{\eta}$ in Eq. (10). To apply the backpropagation method, a loss function $\mathcal{L}(\hat{\mathbf{Y}}, \mathbf{Y})$ is constructed, which defines an error of the predicted dynamic response $\hat{\mathbf{Y}}$ using Eq. (10) and Eq. (11) from the reference measurement data $\mathbf{Y}$. Starting from initial parameter estimates $\boldsymbol{\theta}_0$, the neural network is optimized by taking the gradient descent step to minimize the loss function, which is described as

$$\boldsymbol{\theta}_{i+1} = \boldsymbol{\theta}_i - l_r \frac{\partial \mathcal{L}(\hat{\mathbf{Y}}, \mathbf{Y})}{\partial \boldsymbol{\theta}_i} \quad (12)$$

where l_r is the learning rate, and i denotes the iteration step. The optimal parameters are obtained by achieving the convergence of the iterations.

3.2. *Limitations of applying existing NNAP model to systems with large degree-of-freedoms*

A few limitations exist of NNAP models when applied to systems with large DOFs. First, compared to applications to single DOF systems, a large DOF may significantly increase computational costs for fitting and predictions and lead to a higher chance of overfitting. This is because many equations in Eq. (10) will remain incomplete compared to the cases of small DOFs. Since the neural network in an NNAP model is to compensate for the errors in the incomplete equations, the output dimension of the neural network naturally increases for a structural system with large DOFs. More neurons in each layer and more layers make the training processes of the NNAP model and prediction challenging. Moreover, an excessive number of model parameters may lead to overfitting issues.

Second, an NNAP model needs an initial condition $\mathbf{X}_0$ to initiate the numerical integration of Eq. (10). In general, the measured response $\mathbf{Y}_0$ is available rather than $\mathbf{X}_0$, which may make implementing the NNAP model in practical situations challenging. In the following section, an advanced method for applying the NNAP model to structures with large DOFs is proposed to reduce computational cost and the chance of overfitting and enable the model to predict from the initial measurement $\mathbf{Y}_0$.

4. REDUCED-ORDER NNAP MODEL

4.1. *Description of the proposed model*

To overcome the limitations described in Section 3.2, we propose a reduced-order NNAP model. It is first assumed that the response in the original coordinates $\mathbf{X} = [\boldsymbol{x}^{\mathrm{T}}\ \dot{\boldsymbol{x}}^{\mathrm{T}}]^{\mathrm{T}}$ can be computed from the modal response $\mathbf{Q} = [\boldsymbol{q}^{\mathrm{T}} \quad \dot{\boldsymbol{q}}^{\mathrm{T}}]^{\mathrm{T}}$ as in Section 2.2, i.e.,

$$\mathbf{X} = \mathbf{\Psi}\mathbf{Q} = \begin{bmatrix} \mathbf{\Phi}_{\mathbf{r}} & \mathbf{0} \\ \mathbf{0} & \mathbf{\Phi}_{\mathbf{r}} \end{bmatrix} \mathbf{Q} \tag{13}$$

Substituting Eq. (13) into Eq. (11), the measured response is described as

$$\mathbf{Y} = \mathbf{A}\mathbf{X} = \mathbf{A}\mathbf{\Psi}\mathbf{Q} \tag{14}$$

The reduced-order state-space hybrid model is developed in a form analogous to Eq. (10) as

$$\dot{\mathbf{Q}} = \boldsymbol{\mathcal{P}}_{\mathbf{r}}(\mathbf{Q}, \boldsymbol{p}_{\mathbf{1}}) + \mathbf{R}_{\mathbf{r}}\boldsymbol{\eta}_{\mathbf{r}}(\mathbf{A}\mathbf{\Psi}\mathbf{Q}, \boldsymbol{p}_{\mathbf{2}}; \boldsymbol{\theta}_{\mathbf{r}}) \tag{15}$$

where $\boldsymbol{\mathcal{P}}_{\mathbf{r}}, \mathbf{R}_{\mathbf{r}}, \boldsymbol{\eta}_{\mathbf{r}}$, and $\boldsymbol{\theta}_{\mathbf{r}}$ respectively denote the known dynamics model in modal coordinates, the dummy matrix, the neural network, and its trainable parameters.

Constructing the NNAP model in the reduced-order coordinates is advantageous in that the model requires a relatively lower computational cost and is more robust against overfitting issues. Since the dimension of the NNAP model is reduced from $2N$ to $2N_r$, a smaller neural network can be used to represent unknown dynamics.

4.2. *Prediction and training procedures for the proposed methodology*

To predict the response $\mathbf{X}$ using the reduced-order NNAP model, Eq. (15) is first solved to obtain the modal response $\mathbf{Q}$ using a numerical integration solver (discussed in Section 3.1), given the initial modal response $\mathbf{Q}_0$. Then, the corresponding physical coordinates $\mathbf{X}$ can be obtained from Eq. (13).

The training procedure of the neural network $\boldsymbol{\eta}_{\mathbf{r}}$ is also analogous to the methods described in Section 3.2. The measured response $\hat{\mathbf{Y}}$ is first constructed using Eqs. (14) and (15). The loss function is constructed to represent the error of the predicted response $\hat{\mathbf{Y}}$ with respect to the measured response $\mathbf{Y}$. The neural network in Eq. (15) can be trained by taking the gradient descent step to minimize the loss function.

The initial modal response $\mathbf{Q}_0$ can be obtained from the response at the beginning, i.e., $\mathbf{Y}_0$, as explained in the following. When the dimension of the measured response is larger than that of the modal response, $\mathbf{Q}_0$ can be computed by applying the least squares method to Eq. (14). This procedure is equivalent to multiplying the pseudo-inverse matrix $[\mathbf{A\Psi}]^+$ in Eq. (14), which can be described as

$$\mathbf{Q}_0 = [\mathbf{A\Psi}]^+\mathbf{Y}_0 \tag{16}$$

where $[\ ]^+$ denotes the pseudo-inverse matrix.

4.3. Additional remarks

As explained in Sections 4.1 and 4.2, the proposed model requires a lower computational cost and is more robust against overfitting. Moreover, the model facilitates implementations in practical situations because the processes can start from $\mathbf{Q}_0$ instead of $\mathbf{X}_0$. However, it should be noted that the modal truncation may lead to inaccurate predictions for highly nonlinear systems.

5. NUMERICAL EXAMPLE

5.1. Reference wind load and structural response data

The prediction performance of the proposed NNAP model is tested and demonstrated using a numerical model of the Lysefjord bridge, Norway. We use a part of the finite element (FE) model developed by Wang et al. (2017) to develop an NNAP model. Figure 2 illustrates the bridge configuration and the three directions of the wind velocities, i.e., lateral (u), vertical (w), and longitudinal (v).

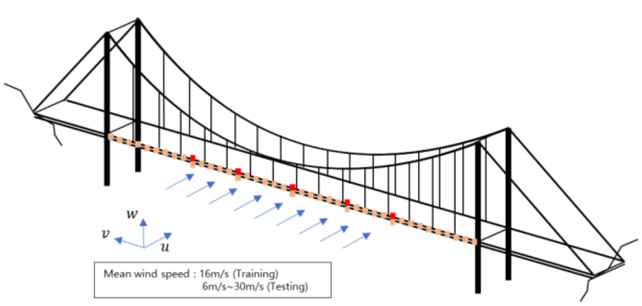

Figure 2: Illustration of the Lysefjord bridge

The bridge structure is described by a total of 123 DOFs, which describe the lateral response $\boldsymbol{x}_u$, vertical response $\boldsymbol{x}_w$, and torsional response $\boldsymbol{x}_t$ at 41 nodes of the deck structure of the main span. The shapes of the first three modes of the main span are shown in Figure 3. Table 1 summarizes the natural frequencies of the first four modes. The reference structure is assumed to have a 5% modal damping ratio.

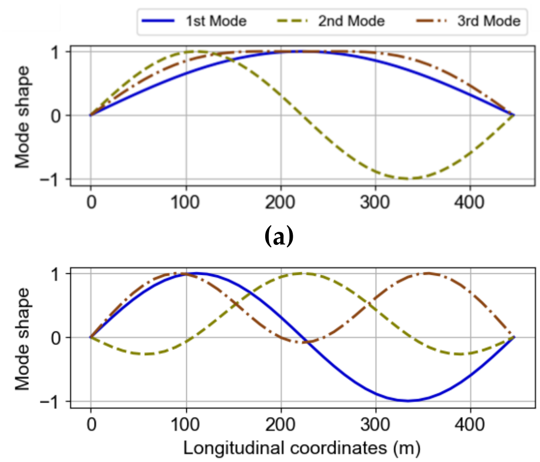

Figure 3:Shapes of the first three modes in (a) lateral and (b) vertical directions

Table 1: Natural frequencies of the first four modes (rad/sec)

Mode / Direction	1	2	3	4
Lateral	*0.81*	*2.78*	*3.50*	*3.75*
Vertical	*1.29*	*2.00*	*2.76*	*3.68*
Torsional	*7.63*	*13.7*	*20.7*	*27.56*

A linear FE model describes the reference structure except for the nonlinearity caused by the response-dependent wind-induced force. In detail, the wind-induced drag force F_D, lift force F_L and torsional moment F_M at each node are respectively described as

$$\begin{aligned} F_D &= \frac{1}{2}\rho C_D(\alpha)HlV_{rel}^2 \\ F_L &= \frac{1}{2}\rho C_L(\alpha)WlV_{rel}^2 \\ F_M &= \frac{1}{2}\rho C_M(\alpha)W^2lV_{rel}^2 \end{aligned} \tag{17}$$

where C_D, C_L, and C_M respectively denote the drag, lift, and moment coefficients, given as the functions of the wind attack angle of the deck α, ρ is the air density, W and H denote the width and height of the deck respectively, l is the length of the deck, i.e., span length, divided by the number of nodes, and V_{rel} is the relative wind speed $V_{rel} = \sqrt{(u - \dot{x}_u)^2 + (w - \dot{x}_z)^2}$. The drag and lift forces are transformed into the force in the lateral direction F_u and that in the vertical direction F_w by

$$\begin{bmatrix} F_u \\ F_w \end{bmatrix} = \begin{bmatrix} \cos(\beta) & -\sin(\beta) \\ \sin(\beta) & \cos(\beta) \end{bmatrix} \begin{bmatrix} F_D \\ F_L \end{bmatrix} \quad (18)$$

where β denotes the angle of the relative wind speed V_{rel}.

As reference data for testing the proposed method, sample time histories of wind speeds in the lateral and vertical directions are generated, while FE analyses obtain the corresponding structural response. Five wind speed time histories are generated from the Kaimal spectrum (Kaimal et al. 1972) to match the lateral mean wind speed of 12, 14, 16, 16, and 22 m/s. Each wind speed time history lasts for 20 minutes, with a sampling rate of 0.01 seconds. Figure 4 shows sample time histories of the wind velocity generated for a mean wind speed of 16m/s.

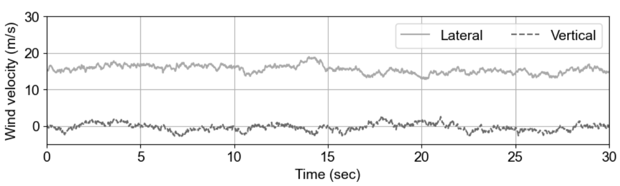

Figure 4: Sample time histories of generated wind velocity (lateral mean wind speed=16m/s)

5.2. NNAP model for target structure and results of training and prediction

5.2.1. Design of the known physics model

The known physics model describes prior information about the dynamics of the system $\boldsymbol{\mathcal{P}}_{\mathbf{r}}(\mathbf{Q}, \boldsymbol{p}_1)$ in the proposed NNAP model. First, the mode shapes $\boldsymbol{\Phi}_{\mathbf{r}}$ of the structure are assumed to be known accurately and used to reduce the dimension of the model. The first four modes in each lateral, vertical, and torsional response are used to construct the reduced-order NNAP model. The corresponding natural frequencies were also given to the known physics model.

Lastly, the simplified input force model is introduced to each node of the proposed NNAP model. In practical situations, the functions of the drag, lift, and moment coefficients, i.e., $C_D(\alpha)$, $C_L(\alpha)$, and $C_M(\alpha)$, are usually unknown unless experiments are available for the structure. Therefore, the input force at each node is assumed as

$$\begin{aligned} F_u &= \frac{1}{2}\rho C_D(0) H l u^2 \\ F_w &= \frac{1}{2}\rho C_L(0) W l w^2 \\ F_M &= 0 \end{aligned} \quad (19)$$

The approximations in Eq. (19) will cause an error in predicting the response by the known physics model. However, if the neural network in the unknown physics model can learn the difference between Eqs. (17) and (18), and Eq. (19), the hybrid model can predict the response accurately.

Combining the physics information described above, the known physics model in the reduced coordinates $\boldsymbol{\mathcal{P}}_{\mathbf{r}}$ is expressed as

$$\boldsymbol{\mathcal{P}}_{\mathbf{r}}(\mathbf{Q}, \boldsymbol{p}_1) = \begin{bmatrix} \dot{\boldsymbol{q}} \\ -\boldsymbol{\Omega}\boldsymbol{q} + \boldsymbol{\Phi}_{\mathbf{r}}^{\mathrm{T}}\mathbf{F}(\boldsymbol{p}_1) \end{bmatrix} \quad (20)$$

where $\boldsymbol{\Omega}$ denotes the diagonal matrix with natural frequencies at each mode, $\mathbf{F}(\boldsymbol{p}_1)$ denotes the input forces at the nodes computed using Eq. (19), and $\boldsymbol{p}_1 = [\boldsymbol{u}^{\mathrm{T}} \;\; \boldsymbol{w}^{\mathrm{T}}]^{\mathrm{T}}$.

5.2.2. Design of the unknown physics model

To complement the model errors induced by Eq. (20), a dummy matrix in Eq. (15), i.e., $\mathbf{R}_{\mathbf{r}}$ is introduced as

$$\mathbf{R}_{\mathbf{r}} = \begin{bmatrix} \mathbf{0} \\ \mathbf{I} \end{bmatrix} \quad (21)$$

where $\mathbf{0}$ denotes a zero matrix and $\mathbf{I}$ denotes an identity matrix. Since the upper half of the equations in Eq. (20), i.e., $\dot{\boldsymbol{q}}$, is already complete, the neural network outputs are introduced only for the lower half of the equations.

The neural network is designed to take the measured response $\mathbf{Y} = \mathbf{A}\boldsymbol{\Psi}\mathbf{Q}$ and the wind speeds $\boldsymbol{u}, \boldsymbol{w}$ as inputs, i.e., $\boldsymbol{p}_2 = [\boldsymbol{u}^{\mathrm{T}} \quad \boldsymbol{w}^{\mathrm{T}}]^{\mathrm{T}}$. The neural network has five hidden layers, each of which has 100~500 neurons, and the exponential linear unit activation function is applied after each hidden layer. Batch normalization is implemented in the first layer. The output dimension of the neural network is 12, which is identical to the number of modes used to reduce the dimension of the NNAP model.

5.3. Training result of the proposed NNAP model

In this example, the responses at 5 locations and the wind speed at 41 locations (visualized by red and orange markers in Figure 2, respectively) are used to train the model. Two sets of wind-induced bridge response data with a mean wind speed of 16m/s are used for training. One set is used to train the model directly, while the other is to select the optimal set of parameters after each epoch. The mean-squared error is calculated to construct the loss function with a learning rate of $l_r = 1 \times 10^{-2}$. Figure 5 shows the training and validation errors at each epoch.

The neural network parameters after 18 epochs, which resulted in the smallest validation error, are selected as the optimal set of parameters. The modal responses predicted for the training data are shown in Figure 6. The results confirm that the proposed NNAP model was trained properly for the modal responses in the lateral and vertical directions. The torsional modes' responses were not as accurate as the others because the torsional responses are relatively small.

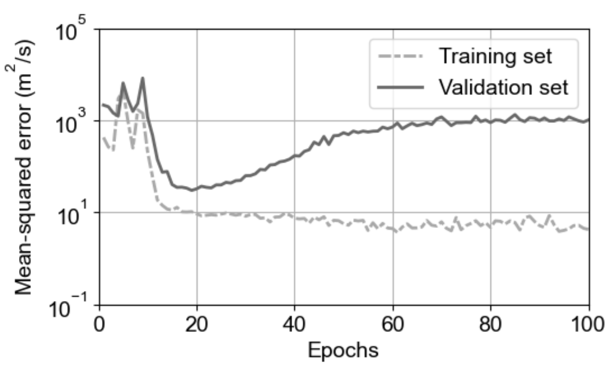

Figure 5:Training and validation errors after each epoch

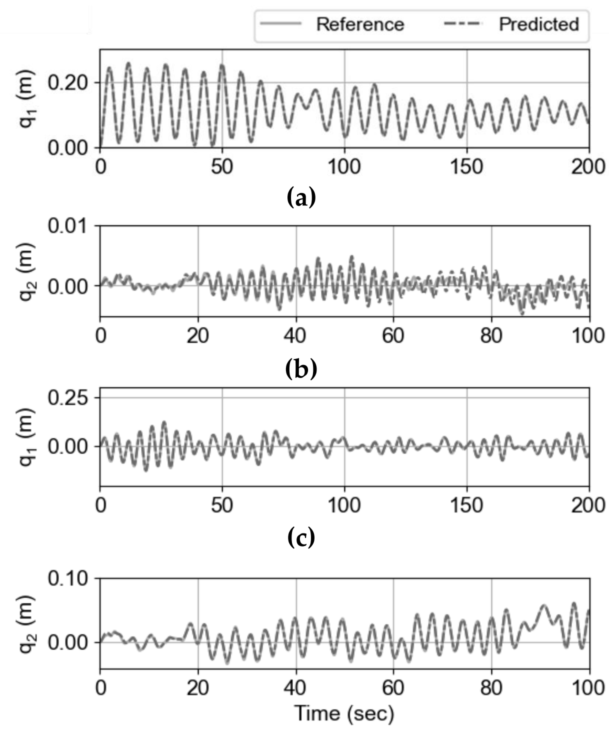

(a)
(b)
(c)
(d)

Figure 6: Modal responses predicted by the proposed model: (a) first lateral, (b) second lateral, (c) first vertical, and (d) second vertical modes

5.4. Testing result of the proposed NNAP model

The wind-induced responses with mean wind speeds of 12, 14, and 22m/s are used to test the performance of the model trained by 16m/s. Figure 7 shows the modal responses in the vertical direction at the mid-span of the bridge. For comparison, the prediction performance by a long short-term memory (LSTM) model (Hochreiter and Schmidhuber 1997) is also shown. The LSTM model is developed with the same training data as the proposed NNAP model and used to predict the vertical responses.

The results in Figure 7 confirm that the proposed NNAP model can successfully incorporate the unknown physics based on measurement data and shows better prediction performance than the LSTM model. It is inferred that the proposed approach performs more efficiently by encoding modal characteristics into the hybrid model. The proposed NNAP model can predict the frequency content of the response successfully because the natural frequencies at the selected modes are also incorporated into the model.

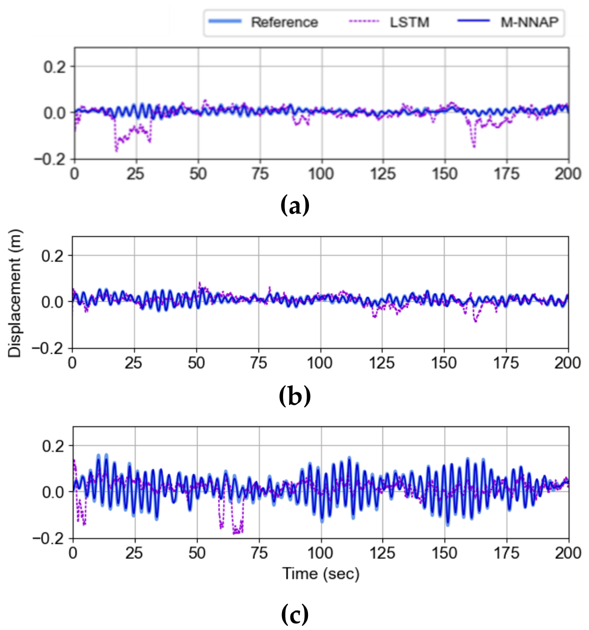

Figure 7: Vertical response prediction at the mid-span of the bridge for mean wind speeds of (a) 12 m/s, (b) 14 m/s, and (c) 22 m/s

6. CONCLUSIONS

A deep-learning-augmented physic model was developed in this study to describe unknown physics by a neural network trained by measurement data. In particular, the neural-network-augmented physics (NNAP) model was further developed to avoid issues in its applications to structures with large degree-of-freedoms (DOFs) through modal truncation. The numerical example of a bridge structure subject to response-dependent wind loads successfully demonstrated the performance of the proposed NNAP model. Despite its successful prediction results, the proposed model may have limitations for highly nonlinear systems in which the mode shapes change significantly. Further research is underway to combine the theory of nonlinear normal modes to facilitate applications of the proposed approach to highly nonlinear MDOF systems.

7. ACKNOWLEDGMENTS

This research was supported by the National Research Foundation of Korea (NRF) Grant funded by the Korean government (NRF-2021R1A2C2003553).

8. REFERENCES

de Groote, W., Kikken, E., Hostens, E., van Hoecke, S., and Crevecoeur, G. (2022). "Neural Network Augmented Physics Models for Systems with Partially Unknown Dynamics: Application to Slider-Crank Mechanism." *IEEE/ASME Transactions on Mechatronics*, 27 (1), 103–114.

Eshkevari, S.S., Takáč, M., Pakzad, S.N., and Jahani, M. (2021). "DynNet: Physics-based neural architecture design for nonlinear structural response modeling and prediction." *Engineering Structures*, 229, 111582.

Hochreiter, S., and Schmidhuber, J. (1997). “Long Short-Term Memory.” *Neural Computation*, 9, 1735–1780.

Kaimal, J.C., Wyngaard, J.C., Izumi, Y., Cote, O.R. (1972). "Spectral characteristics of surface-layer turbulence." *Quarterly Journal of the Royal Meteorological Society*, 98 (417), 563–589.

Kim, J.H., Ghaboussi, J., and Elnashai, A.S. (2012). "Hysteretic mechanical-informational modeling of bolted steel frame connections." *Engineering Structures*, 45, 1–11.

Punjani, A., and Abbeel, P. (2015). "Deep learning helicopter dynamics models." *2015 IEEE International Conference on Robotics and Automation (ICRA).*

Slaats, P.M.A., de Jongh, J., and Sauren, A.A.H.J. (1995). "Model reduction tools for nonlinear structural dynamics." *Computers & Structures*, 54 (6), 1155–1171.

Wang, J., Cheynet, E., Jakobsen, J., and Snæbjörnsson, J. (2017) "Time-domain analysis of wind-induced response of a suspension bridge in comparison with the full-scale measurements." *International Conference on Offshore Mechanics and Arctic Engineering*, 57663.

Zhang, R., Liu, Y., and Sun, H. (2020). "Physics-guided convolutional neural network (PhyCNN) for data-driven seismic response modeling." *Engineering Structures*, 215, 110704.